

Linear stiff string vibrations in musical acoustics: Assessment and comparison of models

Michele Ducceschi^{a)} and Stefan Bilbao

Acoustics and Audio Group, James Clerk Maxwell Building, University of Edinburgh, EH9 3JZ, Edinburgh, United Kingdom

(Received 1 February 2016; revised 12 August 2016; accepted 17 August 2016; published online 10 October 2016)

Strings are amongst the most common elements found in musical instruments and an appropriate physical description of string dynamics is essential to modelling, analysis, and simulation. For linear vibration in a single polarisation, the most common model is based on the Euler–Bernoulli beam equation under tension. In spite of its simple form, such a model gives unbounded phase and group velocities at large wavenumbers, and such behaviour may be interpreted as unphysical. The Timoshenko model has, therefore, been employed in more recent works to overcome such shortcoming. This paper presents a third model based on the shear beam equations. The three models are here assessed and compared with regard to the perceptual considerations in musical acoustics.

© 2016 Acoustical Society of America. [<http://dx.doi.org/10.1121/1.4962553>]

[TRM]

Pages: 2445–2454

I. INTRODUCTION

The simplest model of linear transverse string vibration is almost certainly the one dimensional (1D) wave equation, see for example, the book by Bilbao;¹ normally it is accompanied by additional terms modeling various effects, the most important of which is stiffness, the subject of this paper. Stiffness in strings leads to a progressive stretching or inharmonicity of the partials in the resulting sound, and is essential in any refined model of string vibration, as it leads to perceptually salient effects such as octave stretching, as well as to the reduction of beating phenomena when various notes are played simultaneously.

The most widely used stiff string model is a variant of the 1D wave equation incorporating a stiffness term as per the Euler–Bernoulli model of beam vibration—see Bilbao.¹ Here and henceforth in this article, such a model will be referred to as a stiff string of Euler–Bernoulli type. Such an equation has been employed in a number of studies, especially in the case of finite difference simulations of piano strings. Notable works include those of Ruiz,² Hiller and Ruiz,³ Bacon and Bowsher,⁴ Boutillon,⁵ Chaigne and Askenfelt,⁶ and Giordano.⁷ In the sound synthesis setting, such an equation has also been used as a starting point for digital waveguide models—see Bensa *et al.*⁸ and Ducasse.⁹

The Euler–Bernoulli stiff string model is notable for its simplicity. It is known, however, that for such equation, phase and group velocity are unbounded in the limit of high frequency or wavenumber—see Graff,¹⁰ and it has been noted by some authors that this behaviour is unphysical. To address this shortcoming, more recent work has employed a more refined stiff string model, based on the Timoshenko theory of beams—see the extensive works by Chabassier and associates.^{11–13} The Timoshenko theory can be written as a system of two coupled partial differential equations

(PDEs) of second order, which can be combined into a single equation of fourth order in both space and time. The Timoshenko system is hyperbolic, and predicts finite group velocities; in the low frequency limit, however, the two models converge. The related issue of how large the differences between these two models are, and at which point in the audio spectrum they come into play, has not yet been addressed in the literature in musical acoustics, and the purpose of this article is to analyse and quantify such differences with regard to typical strings as they occur in musical instruments. Timoshenko and Euler–Bernoulli are, of course, only two among a large number of possible models. A third system will be considered here, known as the shear model.

The structure of this article is as follows. Defining parameters for a number of string types which occur in a musical acoustics setting are given in Sec. II. Section III presents the derivation of the Timoshenko model, and two simplified systems that can be derived from it through various levels of simplification: the shear and Euler–Bernoulli models. In Sec. IV, the dispersion relations will be derived for the three models. Boundary conditions and modes will be given in Sec. V. Section VI gives a comparative analysis of the three systems, based on the results derived in Sec. V. Finally, Sec. VII presents a discussion focused on the relative merits of such models in the setting of musical acoustics.

II. MUSICAL STRINGS: REFERENCE CASES

Before proceeding, it is worth introducing a few parameter sets for strings used in musical instruments which will serve as test cases. As the main interest here is in examining the limitations of standard stiff string models, strings for which stiffness effects are at the extreme end of the musical range are chosen here. The case studies are: double-bass E_1 , piano $D_{\#1}$, acoustic guitar E_2 . In the remainder of the paper, they will be denoted as, respectively, E_1^b , $D_{\#1}^p$, and E_2^g . All the strings are made of steel and have circular cross section.

^{a)}Electronic mail: michele.ducceschi@ed.ac.uk

Note that winding is not considered for the strings in this paper. In fact, winding is a technique that allows for an increase of the mass of a string by covering the steel core with a denser metal (usually copper) without changing considerably its stiffness (and thus inharmonicity). As Fletcher points out:¹⁴ “the elastic-restoring torque is due almost entirely to the steel core, but the linear density is due to the core and the windings.” The string parameters are summarised in Table I. In the remainder of the paper, G is the shear modulus, κ is a correction factor known as Timoshenko shear coefficient, I is the area moment of inertia, E is Young’s modulus, T_0 is the applied tension, L_0 is the length of the string and r is the radius. Note that, for isotropic materials, $G = E/2(1 + \nu)$, where ν is Poisson’s ratio ($\nu = 0.3$ for steel), and for strings of circular cross section $\kappa = 6(1 + \nu)/(7 + 6\nu)$ —see Han *et al.*¹⁵ Note that the area A and the area moment of inertia I are readily calculated from r as

$$A = \pi r^2, \quad I = \pi r^4/4.$$

III. MODELS

A stiff string is modelled as a beam under tension in the longitudinal direction, or, in other words, a prestressed rod. In this respect, the stiff string models discussed in this paper must draw from appropriate beam theories.

Exact 3D models have been derived for finite-element applications—see, for example, the works by Jelenić and Crisfield¹⁶ and Betsch and Steinmann.¹⁷ In most cases, however, approximate theories can be used. Approximate models can be derived by averaging out the effects along the cross section, and four such models are prominent in the literature: Timoshenko, shear, Rayleigh and Euler–Bernoulli—see Han *et al.*¹⁵ The Timoshenko model describes the dynamics of both transverse and shear waves, and it can be further simplified to yield the other three models. The validity of the Timoshenko model has been tested in a number of works: Traill-Nash and Collar¹⁸ compare the first two theoretical eigenfrequencies of a thick free–free Timoshenko beam versus experimental results, finding agreement within a 3% range. Davis *et al.*¹⁹ present a solution, using finite elements, of the Timoshenko frequency equations and compare the results versus the exact frequency equations for simply supported and cantilever beams, showing convergence. Renton²⁰ discusses the validity of the Timoshenko model for different values of the *wavelength/beam depth* ratio, concluding that the model is accurate when such ratio larger than 1 (and surely this is the case for musical strings). Stephen²¹ validates and clarifies the results by Renton, for different choices of

TABLE I. Case studies: double-bass string E_1^b , piano string $D_{\#1}^p$ and acoustic guitar string E_2^s . All strings are made of steel, with $\rho = 7860 \text{ kg/m}^3$, $E = 2.02 \times 10^{11} \text{ Pa}$, $G = 7.77 \times 10^{10} \text{ Pa}$ and $\kappa = 0.89$.

	r (mm)	L_0 (m)	T_0 (N)
E_1^b	1.50	1.10	450
$D_{\#1}^p$	0.74	1.94	310
E_2^s	0.71	0.67	150

the shear constant. In turn, there is sufficient evidence that the Timoshenko model constitutes an accurate reference model for the current scope.

It may be written compactly as

$$\begin{aligned} \rho A w_{,tt} &= (A\kappa G + \epsilon_2 T_0)w_{,xx} - (A\kappa G - \epsilon_1 T_0)\phi_{,x}, \\ \rho I \phi_{,tt} &= EI \phi_{,xx} + (A\kappa G - \epsilon_1 T_0)(w_{,x} - \phi). \end{aligned}$$

In the system above, $w(x, t)$ and $\phi(x, t)$ represent, respectively, the transverse displacement and flexural angle for $t \geq 0$ and for $x \in \mathcal{D} \triangleq [0, L_0]$. Indices after a comma represent partial differentiation with respect to t or x . Two distinct forms of the Timoshenko system are encapsulated above, and denoted here as model 1, and 2, which may be selected through the parameters ϵ_1 and ϵ_2 , as

$$(\epsilon_1, \epsilon_2) = \begin{cases} (1, 0) & \text{for Model 1;} \\ (0, 1) & \text{for Model 2.} \end{cases}$$

The system can be scaled to yield a form with fewer free parameters. To this extent, consider the following non-dimensional variables denoted by overbars

$$\bar{w} = \frac{w}{w_0}, \quad \bar{\phi} = \frac{\phi}{\phi_0}, \quad \bar{x} = \frac{x}{x_0}, \quad \bar{t} = \frac{t}{t_0},$$

and the following relations

$$\begin{aligned} x_0^2 &= \frac{I}{A}, \quad t_0^2 = \frac{\rho I}{A\kappa G}, \quad \phi_0 = \frac{w_0}{x_0}, \\ \alpha &= 1 + \frac{T_0}{A\kappa G}, \quad \beta = \frac{E}{\kappa G}. \end{aligned}$$

When rewritten in terms of dimensionless variables (dropping the overbar notation) the Timoshenko system is as follows

$$w_{,tt} = [1 + \epsilon_2(\alpha - 1)]w_{,xx} - [1 - \epsilon_1(\alpha - 1)]\phi_{,x}, \quad (1a)$$

$$\phi_{,tt} = \beta\phi_{,xx} + [1 - \epsilon_1(\alpha - 1)](w_{,x} - \phi). \quad (1b)$$

System (1) is completed by the specification of two initial conditions each for w and ϕ and two boundary conditions for each end of the domain \mathcal{D} . Boundary conditions will be considered in depth in Sec. V.

The Timoshenko system may be arrived at by means of different techniques. One may choose to draw a free body diagram and balance moments and forces; alternatively one may derive the kinetic and potential energies from elasticity theory considerations, and perform a variational analysis. The latter approach is briefly recalled here, whereby the equations of motion through standard variational approaches, with the various kinetic and potential energy components expressible as appropriate quadratic forms.

Assuming regularity of the source term and of the initial conditions, as well as a set of energy-conserving boundary conditions (see Sec. V), a strong solution to the system exists over the domain $x \in \mathcal{D}$ (see, for instance, Chabassier *et al.*¹¹). Hence, w , ϕ , and their derivatives up to the order 2

necessarily belong to a set $V : \mathcal{D} \times \mathbb{R}^+$ such that $v(x, t) \in V \subseteq \mathcal{C}^0(\mathcal{D}; \mathbb{R}^+)$ and $v(x, t) \in L^2(\mathcal{D})$. It is then possible to define, for two functions $v_1, v_2 \in V$, the following scalar product and norm

$$\langle v_1, v_2 \rangle = \int_0^L v_1 v_2 dx, \quad \|v_1\|^2 = \langle v_1, v_1 \rangle.$$

Using the above notation, the Hamiltonian for the prestressed Timoshenko beam, $\mathcal{H}_{\text{TM}}^{(1),(2)}$, is

$$\begin{aligned} \mathcal{H}_{\text{TM}}^{(1),(2)} = & \underbrace{\frac{\|w_{,t}\|^2}{2}}_{\mathcal{K}_b} + \underbrace{\frac{\|\phi_{,t}\|^2}{2}}_{\mathcal{K}_s} + \underbrace{\frac{\beta \|\phi_{,x}\|^2}{2}}_{\mathcal{U}_b} + \underbrace{\frac{\|\phi - w_{,x}\|^2}{2}}_{\mathcal{U}_s} \\ & + \epsilon_1 \underbrace{\frac{\alpha - 1}{2} [\langle w_{,x}, \phi \rangle - \|\phi\|^2]}_{\mathcal{U}_t^{(1)}} + \epsilon_2 \underbrace{\frac{\alpha - 1}{2} \|w_{,x}\|^2}_{\mathcal{U}_t^{(2)}}. \end{aligned} \quad (2)$$

It is composed of kinetic ($\mathcal{K}_{\text{TM}} \triangleq \mathcal{K}_s + \mathcal{K}_b$) and potential ($\mathcal{U}_{\text{TM}}^{(1),(2)} \triangleq \mathcal{U}_s + \mathcal{U}_b + \mathcal{U}_t^{(1),(2)}$) energy terms, where the subscripts b,s,t stand for “bending,” “shear,” and “tension,” respectively. (Notice, however, that $\mathcal{U}_t^{(1)}$ is not by definition positive; hence the term “energy” is used in this case with a little abuse of language. See also the remark at the end of this section). The Lagrangian \mathcal{L}_{TM} may be written as

$$\mathcal{L}_{\text{TM}}^{(1),(2)} = \mathcal{K}_{\text{TM}} - \mathcal{U}_{\text{TM}}^{(1),(2)},$$

and, under standard variational procedures, leads to system (1).

Before introducing the boundary conditions, the question of which of the two models one should use must be addressed. A literature survey reveals that the choice of one model over the other is still matter of debate: Kounadis²² was the first author to address the problem of a prestressed

Timoshenko beam in depth, using both free-body diagrams and conservative methods: surprisingly, these different approaches gave rise to two distinct models, with the former producing model 1, and the latter model 2. He also concluded that model 1 “cannot be derived by means of a variational (energy) method.” However, it was later shown by Sato²³ that both models can indeed be written in terms of Hamilton’s principle, with energy components as per Eq. (2). Later, Djondjorov and Vassilev²⁴ investigated numerically the onset of buckling for the two models, and pointed out that further experimental verification was needed to identify the model which predicts the “critical load” (i.e., the load at which buckling takes place) more accurately.

Turning the attention now to musical strings, one may observe that typical tensions are far from being “critical”: for the strings in Table I the ratio $T_0/A\kappa G$ is on the order of 10^{-3} , small compared to the values by Djondjorov and Vassilev²⁴ (on the order of 1). It is interesting to plot the phase and group velocities, c_p and c_g , versus the wavenumber γ for the thick E_1^b string of Table I, for both model 1 and model 2. This is done in Figs. 1(a) and 1(b), showing a nearly total overlap; for a more quantitative comparison, one may refer to Figs. 1(c) and 1(d) for plots of the relative deviation of the two models, for both the phase and group velocities, and conclude that such deviation is much less than one part over one thousand over an interval of wavenumbers which extends well beyond the audible range. As a result, the two models in the context of musical acoustics are perceptually indistinguishable.

Model 2 has recently been used by Chabassier *et al.*¹² to model and simulate the strings of grand-piano. This choice is partly justified by the positive-definiteness of the quadratic form $\mathcal{U}_t^{(2)}$ in Eq. (2), as opposed to $\mathcal{U}_t^{(1)}$, which is of indeterminate sign. Such choice will be enforced here as well, and hence for the remainder of the paper model 1 will be disregarded.

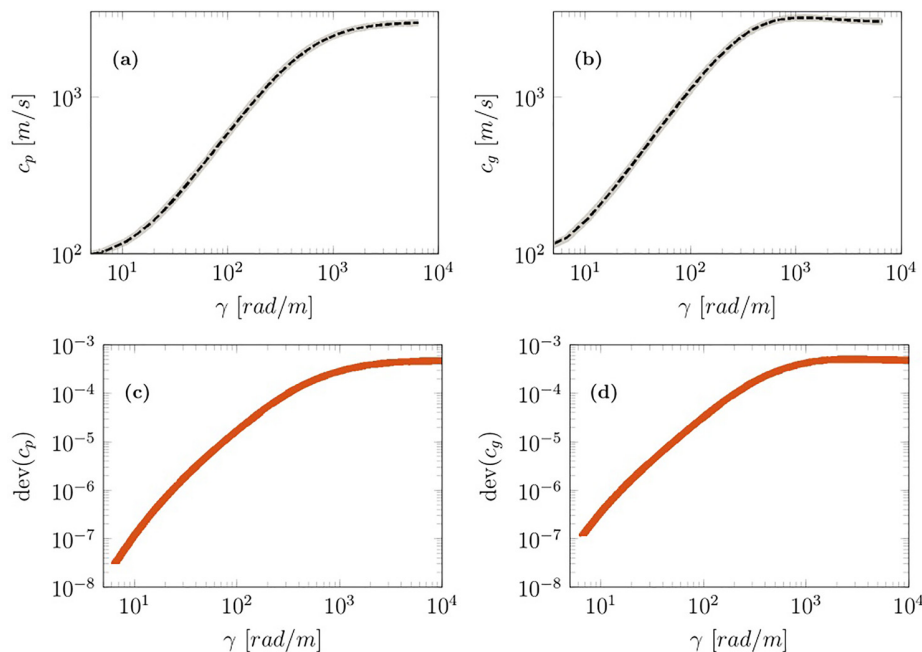


FIG. 1. (Color online) The double-bass E_1^b string. Comparison of prestressed Timoshenko models, as per (1). (a) Phase velocity of model 1 (thick line) and model 2 (dashed line). (b) Group velocity of model 1 (thick line) and model 2 (dashed line). (c) Relative difference of the phase velocities for model 1 and model 2, defined as $\text{dev}(c_p) = 2|c_p^{(1)} - c_p^{(2)}| / |c_p^{(1)} + c_p^{(2)}|$. (d) Relative difference of the group velocities for model 1 and model 2, defined as $\text{dev}(c_g) = 2|c_g^{(1)} - c_g^{(2)}| / |c_g^{(1)} + c_g^{(2)}|$.

A. Timoshenko's model

Summarising, the prestressed *Timoshenko* system (TM), in its scaled form, is

$$w_{,tt} = \alpha w_{,xx} - \phi_{,x}; \quad (3a)$$

$$\phi_{,tt} = \beta \phi_{,xx} + w_{,x} - \phi, \quad (3b)$$

and the associated Hamiltonian is

$$\mathcal{H}_{\text{TM}} = \underbrace{\frac{\|w_{,t}\|^2}{2} + \frac{\|\phi_{,t}\|^2}{2}}_{\mathcal{K}_{\text{TM}}} + \underbrace{\frac{\beta\|\phi_{,x}\|^2}{2} + \frac{\|\phi - w_{,x}\|^2}{2} + \frac{\alpha - 1}{2}\|w_{,x}\|^2}_{\mathcal{U}_{\text{TM}}}.$$

Notice that Eq. (3) can be reduced to a single fourth-order, hyperbolic equation in w ,

$$w_{,ttt} - (\alpha + \beta)w_{,ttx} + \alpha\beta w_{,xxx} - (\alpha - 1)w_{,xx} + w_{,tt} = 0. \quad (4)$$

B. Shear model

The Timoshenko model can be simplified in a number of ways to yield simpler systems. One such model of interest here is known as the *shear* model and is derived by neglecting the rotational inertia in Eq. (3b) (see Han *et al.*¹⁵). In fact, the shear model may be arrived at by considering the asymptotic solution of Timoshenko for large wavelengths, as shown by Hodges.²⁵ The validity of such an assumption was later challenged by Aristizabal-Ochoa,²⁶ who pointed out that the shear beam with at least one free end and at most one rotationally constrained end invalidates the conservation of angular momentum, as proven by Kausel.²⁷ For musical acoustics, however, strings are fixed and, therefore, the shear model is a valid approximation to Timoshenko. The prestressed shear system (SH) may be written as

$$w_{,tt} = \alpha w_{,xx} - \phi_{,x}; \quad (5a)$$

$$0 = \beta \phi_{,xx} + w_{,x} - \phi. \quad (5b)$$

In this system, the shear force is still taken into account but the absence of rotational inertia forbids the development of shear waves. The associated Hamiltonian is obtained from the Timoshenko system by removing the kinetic rotational energy. Hence,

$$\mathcal{H}_{\text{SH}} = \underbrace{\frac{\|w_{,t}\|^2}{2}}_{\mathcal{K}_{\text{SH}}} + \underbrace{\frac{\beta\|\phi_{,x}\|^2}{2} + \frac{\|\phi - w_{,x}\|^2}{2} + \frac{\alpha - 1}{2}\|w_{,x}\|^2}_{\mathcal{U}_{\text{SH}}}.$$

As before, Eq. (5) may be consolidated into a single equation in w :

$$w_{,tt} - \beta w_{,ttx} = (\alpha - 1)w_{,xx} - \alpha\beta w_{,xxx}. \quad (6)$$

C. Euler–Bernoulli model

The *Euler–Bernoulli* (EB) model is obtained from the shear model in the following way. Substitute $\phi = e^{j(\omega t - \gamma x)}$ into Eq. (5b) to obtain $\phi = w_{,x}/(\gamma^2\beta + 1)$. Expanding the denominator in the limit of small wavelengths γ gives $\phi \approx (1 - \gamma^2\beta)w_{,x}$. In the time domain, the corresponding relation is $\phi = w_{,x} - \beta w_{,xxx}$. This relation is then substituted into Eq. (5a) to obtain

$$w_{,tt} - (\alpha - 1)w_{,xx} + \beta w_{,xxx} = 0. \quad (7)$$

For the Euler–Bernoulli model, the Hamiltonian is

$$\mathcal{H}_{\text{EB}} = \underbrace{\frac{\|w_{,t}\|^2}{2}}_{\mathcal{K}_{\text{EB}}} + \underbrace{\frac{(\alpha - 1)\|w_{,x}\|^2}{2} + \frac{\beta\|w_{,xxx}\|^2}{2}}_{\mathcal{U}_{\text{EB}}}.$$

Before proceeding with Sec. IV, it is worth mentioning a fourth popular beam model, known as the *Rayleigh* model, which is obtained from the Euler–Bernoulli model by adding rotatory inertia. The Rayleigh model will not be discussed in detail here. This choice is justified by the relative importance of the shear term over the rotatory inertia term. As Han *et al.* point out:¹⁵ “[It is established that] for a typical material and cross section, the shear term is roughly 3–6 times larger than the rotary term.” Hence, the Rayleigh model will be discarded from now on.

IV. DISPERSION RELATIONS

Stiff strings are dispersive. The dispersion relations for the present models are obtained by examining the behaviour of a monochromatic solution of frequency ω and wavenumber γ , thus extracting a characteristic equation. The monochromatic solution is of the form

$$w = e^{j(\omega t - \gamma x)}.$$

When substituted into either Eqs. (4), (6), or (7), the characteristic equations are recovered. They are now presented and discussed.

A. Timoshenko's model

For model (4), the characteristic equation is

$$\omega^4 + (-\alpha\gamma^2 - \beta\gamma^2 - 1)\omega^2 + \alpha\gamma^2 - \gamma^2 + \alpha\beta\gamma^4 = 0.$$

This is a fourth order equation in ω , for which solutions may be written as

$$\omega_{\pm}^2 = \frac{(\alpha + \beta)\gamma^2 + 1}{2} \pm \frac{\left((1 + (\beta - \alpha)\gamma^2)^2 + 4\gamma^2\right)^{1/2}}{2}.$$

Notice that the Timoshenko system possesses *two* different dispersion curves, which will be indicated here as (+)

and (-). The graphs of these curves (for the E_1^b string) are plotted in Fig. 2.

In the small and large wavenumber limits, one has

$$\lim_{\gamma \rightarrow 0} \omega_{\pm}^2 = \begin{cases} 1 + (\beta + 1)\gamma^2 \\ (\alpha - 1)\gamma^2, \end{cases} \quad \lim_{\gamma \rightarrow \infty} \omega_{\pm}^2 = \begin{cases} \beta\gamma^2 \\ \alpha\gamma^2. \end{cases}$$

The limits of the phase and group velocities are also of interest. The phase and group velocities are defined as

$$c_p = \frac{\omega}{\gamma}, \quad c_g = \frac{d\omega}{d\gamma}.$$

The phase velocity has the following limiting values:

$$\lim_{\gamma \rightarrow 0} c_{p\pm} = \begin{cases} \infty \\ (\alpha - 1)^{1/2}, \end{cases} \quad \lim_{\gamma \rightarrow \infty} c_{p\pm} = \begin{cases} \beta^{1/2} \\ \alpha^{1/2}. \end{cases}$$

Note that, although for both (+) and (-) the phase velocities are bounded at infinity, the phase velocity of (+) is unbounded for small wavenumbers. The limits for the group velocities are readily obtained as

$$\lim_{\gamma \rightarrow 0} c_{g\pm} = \begin{cases} (\beta + 1)^{1/2} \\ (\alpha - 1)^{1/2}, \end{cases} \quad \lim_{\gamma \rightarrow \infty} c_{g\pm} = \begin{cases} \beta^{1/2} \\ \alpha^{1/2}. \end{cases}$$

Hence the group velocity is always bounded. This property of bounded limiting group velocity has motivated the use of the Timoshenko model for musical acoustics, see, for example, Chabassier *et al.*¹¹ Notice in particular, though, that for strings of musical interest, one of the solution curves (+) lies well outside the audio range.

B. Shear model

For model (6), the characteristic equation is

$$\omega^2 = \frac{\gamma^2(\alpha\beta\gamma^2 + \alpha - 1)}{\beta\gamma^2 + 1}.$$

Again, asymptotic solutions are sought in the small and large wavenumber limits:

$$\lim_{\gamma \rightarrow 0} \omega^2 = (\alpha - 1)\gamma^2, \quad \lim_{\gamma \rightarrow \infty} \omega^2 = \alpha\gamma^2.$$

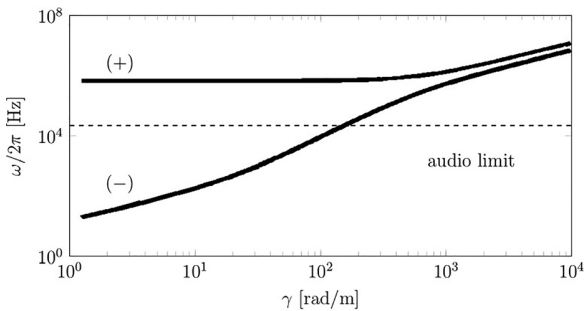


FIG. 2. Double-bass E_1^b . Dispersion relations (+) and (-) for the prestressed Timoshenko system. Audible range below dashed line.

These limits yield the following phase and group velocities

$$\lim_{\gamma \rightarrow 0} [c_p, c_g] = (\alpha - 1)^{1/2}, \quad \lim_{\gamma \rightarrow \infty} [c_p, c_g] = \alpha^{1/2}.$$

Notice that these are the same asymptotes as the (-) branch of the Timoshenko model, which is that which is of primary interest in musical acoustics.

C. Euler–Bernoulli model

For Eq. (7), the dispersion relation is readily obtained as

$$\omega^2 = \gamma^2[(\alpha - 1) + \gamma^2\beta].$$

In this case one sees immediately that

$$\lim_{\gamma \rightarrow 0} \omega^2 = (\alpha - 1)\gamma^2, \quad \lim_{\gamma \rightarrow \infty} \omega^2 = \infty. \\ \lim_{\gamma \rightarrow 0} [c_p, c_g] = (\alpha - 1)^{1/2}, \quad \lim_{\gamma \rightarrow \infty} [c_p, c_g] = \infty.$$

At low frequencies, the behaviour is the same as for the shear and Timoshenko models. However, both phase and group velocities become unbounded at high frequencies. Such characteristic is of course an anomaly, and has been suggested as a reason for using thick beam theories in musical acoustics applications.

V. BOUNDARY CONDITIONS AND MODES

The dispersion relations obtained in Sec. IV are valid for waves travelling on unbounded strings. When boundaries are considered, particular solutions in the form of *standing waves* appear in the systems. The relation between the frequency of oscillation and the (complex) wavenumber of the standing wave can be obtained for a given model by considering

$$w = e^{j\omega t} e^{rx},$$

with $\omega \in \mathbb{R}$ and $r \in \mathbb{C}$. Inserting such solution into either Eqs. (4), (6), or (7), one obtains characteristic equations to be solved for r . Such equations are fourth-order in r with solutions (r_1, r_2, r_3, r_4) and, therefore, a standing wave has the general form

$$w = e^{j\omega t} \Psi(x), \tag{8}$$

with

$$\Psi(x) = d_1 e^{r_1 x} + d_2 e^{r_2 x} + d_3 e^{r_3 x} + d_4 e^{r_4 x}. \tag{9}$$

It is anticipated that for the three models in this paper, the complex wavenumbers (r_1, r_2, r_3, r_4) are such that

$$r_1, r_2 \in \mathbb{R}, \quad r_1 = -r_2; \\ r_3, r_4 \in i\mathbb{R}, \quad r_3 = -r_4.$$

For this reason, the modal frequencies can be expressed as

$$\Psi = d_1 \sin(\lambda_- x) + d_2 \cos(\lambda_- x) + d_3 \sinh(\lambda_+ x) + d_4 \cosh(\lambda_+ x), \quad (10)$$

where $\lambda_+ = \sqrt{r_1^2}$, $\lambda_- = \sqrt{|r_3^2|}$.

The coefficients $\mathbf{d} \triangleq (d_1, d_2, d_3, d_4)^T$ are not independent. They are found by inserting Eq. (8) into the prescribed boundary conditions. This gives an equation of the form

$$\mathbf{A} \mathbf{d} = \mathbf{0}, \quad (11)$$

where \mathbf{A} is a 4×4 matrix. Nontrivial solutions exist when the determinant of \mathbf{A} vanishes.

In the following subsections, the characteristic equations and boundary conditions will be given and discussed for the Timoshenko, shear, and Euler–Bernoulli models.

A. Timoshenko’s model

Boundary conditions for the prestressed Timoshenko system may be obtained by varying the Lagrangian. Classical simply supported (SS), clamped (CL), and free (FF) conditions are recovered as

$$\begin{aligned} \text{SS} : \quad w = \phi_{,x} = 0, \quad \text{CL} : \quad w = \phi = 0, \\ \text{FF} : \quad \alpha w_{,x} - \phi = \phi_{,x} = 0. \end{aligned} \quad (12)$$

The simply supported conditions describe a fixed edge with vanishing moment ($\phi_{,x}$). For the clamped case, the edge and the cross section are fixed (therefore, these conditions are purely geometrical); for the free case both the moment and the shear force vanish. The boundary conditions for the equivalent fourth-order Eq. (4) are summarised in Table II.

The characteristic equation for the complex wavenumber r is

$$\alpha \beta r^4 + r^2[(\alpha + \beta)\omega^2 - \alpha + 1] + \omega^4 - \omega^2 = 0,$$

with solutions

$$\begin{aligned} 2\alpha\beta r_{\pm}^2 = \alpha - 1 - (\alpha + \beta)\omega^2 \pm \left[(\alpha - \beta)^2 \omega^4 \right. \\ \left. + 2(\alpha + \beta + \alpha\beta - \alpha^2)\omega^2 + (\alpha - 1)^2 \right]^{1/2} \\ \triangleq P_1(\omega^2) \pm [P_2(\omega^2)]^{1/2}. \end{aligned}$$

One can prove that $P_2(\omega^2) > 0 \forall \omega^2 \in \mathbb{R}^+$, and thus $r_{\pm}^2 \in \mathbb{R} \forall \omega^2 \in \mathbb{R}^+$. Turning on the sign of r_{\pm}^2 , one has

TABLE II. Summary of classical boundary conditions for the Timoshenko, shear and Euler–Bernoulli models. All quantities in the table vanish at the boundary.

	SS	CL	FF
TM	w	w	$-(\alpha + \beta)w_{,ttx} + (1 - \alpha)w_{,x} + \alpha\beta w_{,xxx}$
	$w_{,xx}$	$\alpha\beta w_{,xxx} + w_{,x} - \beta w_{,xtt}$	$w_{,tt} - \alpha w_{,xx}$
SH	w	w	$-\beta w_{,ttx} + (1 - \alpha)w_{,x} + \alpha\beta w_{,xxx}$
	$w_{,xx}$	$\alpha\beta w_{,xxx} + w_{,x} - \beta w_{,xtt}$	$w_{,tt} - \alpha w_{,xx}$
EB	w	w	$(1 - \alpha)w_{,x} + \beta w_{,xxx}$
	$w_{,xx}$	$w_{,x}$	$w_{,xx}$

	$\omega^2 \leq 1$	$\omega^2 > 1$
r_+^2	≥ 0	< 0
r_-^2	≤ 0	< 0

The solutions for $\omega^2 > 1$ are in essence the discrete equivalent of the (+) branch in Fig. 2. Solutions corresponding to the (−) branch (which is the branch of interest in musical acoustics) are obtained for $\omega^2 \leq 1$. The general solution for the modes is of the form of Eq. (10), with $\lambda_+ = \sqrt{r_+^2}$, $\lambda_- = \sqrt{|r_-^2|}$. Solving Eq. (11) for the selected boundary conditions gives a transcendental equation which must be solved numerically. A summary of such frequency equations for the classic boundary conditions is given in Table III.

B. Shear model

For the shear model, boundary conditions may be determined, again using variational methods, as follows

$$\begin{aligned} \text{SS} : \quad w = \phi_{,x} = 0, \quad \text{CL} : \quad w = \phi = 0, \\ \text{FF} : \quad \alpha w_{,x} - \phi = \phi_{,x} = 0. \end{aligned} \quad (13)$$

Note that these are formally identical to those for the Timoshenko system. The boundary conditions in the sole variable w , however, are different (see Table II).

Substitution of Eq. (8) into Eq. (5) gives the characteristic equation in r

$$\alpha \beta r^4 + r^2[\beta \omega^2 - \alpha + 1] - \omega^2 = 0,$$

with solutions

$$\begin{aligned} 2\alpha\beta r_{\pm}^2 = \alpha - 1 \\ - \beta \omega^2 \pm \left[\beta^2 \omega^4 + 2\beta(\alpha + 1)\omega^2 + (\alpha - 1)^2 \right]^{1/2}. \end{aligned}$$

In this case $r_+^2 > 0 \forall \omega^2 \in \mathbb{R}^+$ and $r_-^2 < 0 \forall \omega^2 \in \mathbb{R}^+$. Hence, as for the Timoshenko case, the modal functions are of the form Eq. (10) with $\lambda_+ = \sqrt{r_+^2}$, $\lambda_- = \sqrt{|r_-^2|}$. Solving Eq. (11) for the selected boundary conditions leads to the transcendental frequency equations given in Table III.

C. Euler–Bernoulli model

Boundary conditions are again obtained through a variational approach. The result is

$$\begin{aligned} \text{SS} : \quad w = w_{,xx} = 0, \quad \text{CL} : \quad w = w_{,x} = 0, \\ \text{FF} : \quad w_{,xx} = (1 - \alpha)w_{,x} + \beta w_{,xxx} = 0. \end{aligned} \quad (14)$$

TABLE III. General form for the frequency equations for a prestressed Timoshenko, shear or Euler–Bernoulli beams, for the classical simply supported, clamped and free end conditions. The coefficients C_{cl} , C_{ff} have lengthy expressions and are, therefore, given in the Appendix.

SS	$\sin(\lambda_- L) \sinh(\lambda_+ L) = 0$
CL	$C_{cl} \sin(\lambda_- L) \sinh(\lambda_+ L) - \cos(\lambda_- L) \cosh(\lambda_+ L) + 1 = 0$
FF	$C_{ff} \sin(\lambda_- L) \sinh(\lambda_+ L) - \cos(\lambda_- L) \cosh(\lambda_+ L) + 1 = 0$

The characteristic equation is

$$r_{\pm}^2 = \frac{(\alpha - 1) \pm [(\alpha - 1)^2 + 4\beta\omega^2]^{1/2}}{2\beta}.$$

Clearly $r_+^2 > 0 \forall \omega^2 \in \mathbb{R}^+$ and $r_-^2 < 0 \forall \omega^2 \in \mathbb{R}^+$ and so the modal function Ψ can be written again as Eq. (10) where $\lambda_+ = \sqrt{r_+^2}$, $\lambda_- = \sqrt{|r_-^2|}$. Inserting this solution into the chosen boundary conditions in Table II gives the transcendental frequency equations given in Table III.

VI. ANALYSIS

Now that the equations, dispersion relations and modes have been formally derived for the three models, a quantitative analysis is provided, to assess the differences amongst the models for the specific cases of Table I. First, dispersion curves, phase and group velocities will be plotted and analysed; second, a few modes will be calculated and compared.

A. Dispersion curves

Dispersion curves are now presented for the strings of parameters as given in Table I.

Figure 3 shows the dispersion relations, phase and group velocities for the low piano string, $D_{\#1}^p$. Note in particular, that the phase and group velocities [Figs. 3(b) and 3(c)] of the Timoshenko and shear models do attain the same limit at large wavenumbers (i.e., $\alpha^{1/2}$), as shown in Sec. IV, while for the Euler–Bernoulli model, they diverge. In the limit of small wavenumbers the three models show good agreement. The horizontal line in Fig. 3(a) represents the limit of human hearing (20 kHz); this is the upper limit of interest in musical acoustics. Undoubtedly, frequencies for the Euler–Bernoulli and shear models are somewhat higher than for the Timoshenko system, but the differences are small for audio frequencies. To quantify the deviation from the Timoshenko model, relative deviations for the frequencies and group velocities are defined in the following way

$$\begin{aligned} \text{dev}_{\omega_{EB}, \omega_{SH}} &= \sup_{[0, \bar{\gamma}]} \left| \frac{\omega_{EB, SH}}{\omega_{TM}} - 1 \right|, \\ \text{dev}_{c_{gEB}, c_{gSH}} &= \sup_{[0, \bar{\gamma}]} \left| \frac{c_{gEB, SH}}{c_{gTM}} - 1 \right|, \end{aligned} \quad (15)$$

where $\bar{\gamma}$ is the wavenumber corresponding the upper limit of human hearing in the Timoshenko model ($\bar{\gamma} \sim 254$ rad/m for $D_{\#1}^p$, as seen in Fig. 3), and “sup” indicates the supremum (although in all cases sup is found at $\bar{\gamma}$). Note that the deviation of the phase velocity is necessarily equal to the deviation of the frequencies and, therefore, it is not calculated. With these definitions, one obtains

$$\begin{aligned} \text{dev}_{\omega_{EB}} &= 0.016, \quad \text{dev}_{c_{gEB}} = 0.034, \\ \text{dev}_{\omega_{SH}} &= 0.004, \quad \text{dev}_{c_{gSH}} = 0.008. \end{aligned}$$

For a given model, the deviation of the group velocity is larger than the deviation of the phase velocity by a factor close to 2 and the shear model is more accurate than the

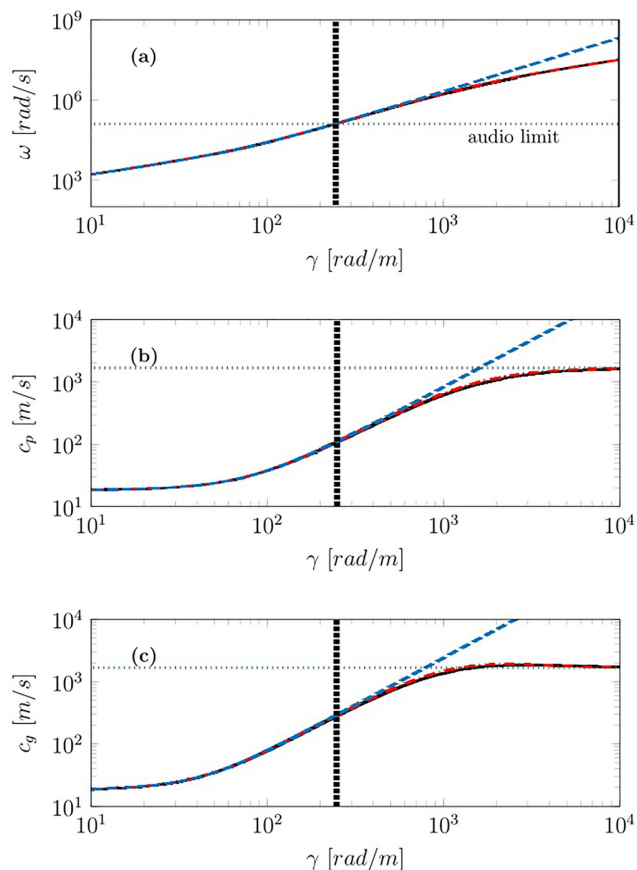


FIG. 3. (Color online) The piano $D_{\#1}^p$ string. For all figures, the vertical dashed line is the upper limit of human hearing. TM is represented by a solid line, SH by a dashed-dotted line, EB by a dashed line. (a) Dispersion relation; horizontal dotted line is upper limit of human hearing. (b) Phase velocity; horizontal dotted line is the limiting velocity for the shear and Timoshenko models, $\bar{c}_p = \alpha^{1/2}$; (c) group velocity; horizontal dotted line is the limiting velocity for the shear and Timoshenko models, $\bar{c}_g = \alpha^{1/2}$.

Euler–Bernoulli model by a factor close to 4. Note that the deviation for ω , calculated in cents, gives

$$\text{cdev} \triangleq 1200 \log_2 \frac{\omega_{EB, SH}}{\omega_{TM}} = \begin{cases} 27.6 \text{ cents for EB;} \\ 7.20 \text{ cents for SH.} \end{cases}$$

This is a little more than a quarter of a semitone for the Euler–Bernoulli model and a quarter of that for the shear model.

For the E_1^b string of the double-bass the deviations as defined in Eq. (15) (with $\bar{\gamma} \sim 184$ rad/m) are

$$\begin{aligned} \text{dev}_{\omega_{EB}} &= 0.036, \quad \text{dev}_{c_{gEB}} = 0.073, \\ \text{dev}_{\omega_{SH}} &= 0.008, \quad \text{dev}_{c_{gSH}} = 0.016. \end{aligned}$$

Note in particular, that for the piano string $D_{\#1}^p$ both the Euler–Bernoulli and shear models are closer to the Timoshenko system than the double-bass string E_1^b : this is in accordance with the fact that the piano string is slenderer than the double-bass string (i.e., the ratio between the radius and the length is smaller for $D_{\#1}^p$ than for E_1^b). Deviations in cents are

$$\text{cdev} = \begin{cases} 61.5 \text{ cents for EB;} \\ 14.7 \text{ cents for SH;} \end{cases}$$

which shows that the maximum deviation over the range of audible frequencies is about half a semitone for the Euler–Bernoulli model and one sixth of a semitone for the shear model.

For the guitar E_2^g string, with $\bar{\gamma} \sim 255 \text{ rad/m}$

$$\begin{aligned} \text{dev}_{\omega\text{EB}} &= 0.015, \quad \text{dev}_{c_g\text{EB}} = 0.031, \\ \text{dev}_{\omega\text{SH}} &= 0.004, \quad \text{dev}_{c_g\text{SH}} = 0.008. \end{aligned}$$

Deviations in cents are

$$\text{cdev} = \begin{cases} 26.1 \text{ cents for EB;} \\ 6.70 \text{ cents for SH,} \end{cases}$$

similar to those for the $D_{\#1}^p$ string.

B. Modal frequencies

The frequency equations in Table III can be solved using an appropriate root finder method, for instance the Newton-Raphson method. Table IV presents a few eigenfrequencies for fixed conditions for the three strings, comparing the three models. Note that, for simply supported conditions and in the case of the Euler–Bernoulli model, the results in the Table are consistent with the well known formula for inharmonicity, i.e.,

TABLE IV. Collection of a few eigenfrequencies under clamped and simply supported conditions, comparison of TM, SH, EB over the three strings under study. Note that for 50 and 100 the frequencies in the table must be multiplied by 10^3 . Values in Hz.

Mode	Clamped			S. Supported			
	E_1^b	$D_{\#1}^p$	E_2^g	E_1^b	$D_{\#1}^p$	E_2^g	
1	44.63	39.43	86.36	41.20	38.93	81.85	TM
	44.63	39.43	86.36	41.20	38.93	81.85	SH
	44.63	39.43	86.36	41.20	38.93	81.85	EB
10	684.5	402.1	1109	640.7	396.9	1.055	TM
	684.7	402.1	1110	640.8	397.0	1.055	SH
	685.1	402.1	1110	641.1	397.0	1.055	EB
$50 (\times 10^3)$	12.47	2.782	17.30	12.24	2.750	17.00	TM
	12.54	2.784	17.37	12.31	2.751	17.05	SH
	12.75	2.786	17.55	12.51	2.753	17.22	EB
$100 (\times 10^3)$	46.10	8.727	64.50	45.72	8.656	63.93	TM
	46.91	8.742	65.30	46.53	8.671	64.72	SH
	50.02	8.780	68.08	49.53	8.707	67.40	EB

$$f_n = n f_1 \sqrt{\frac{\alpha - 1 + \beta(n\pi/L)^2}{\alpha - 1 + \beta(\pi/L)^2}}.$$

The modal frequencies for the piano $D_{\#1}^p$ string are plotted in Fig. 4, for the three models. It is seen that for low mode numbers the eigenfrequencies are coincident, and they start to deviate as the mode number is increased.

Figure 5 shows the deviation in cents of the shear and Euler–Bernoulli models from the Timoshenko system, over a

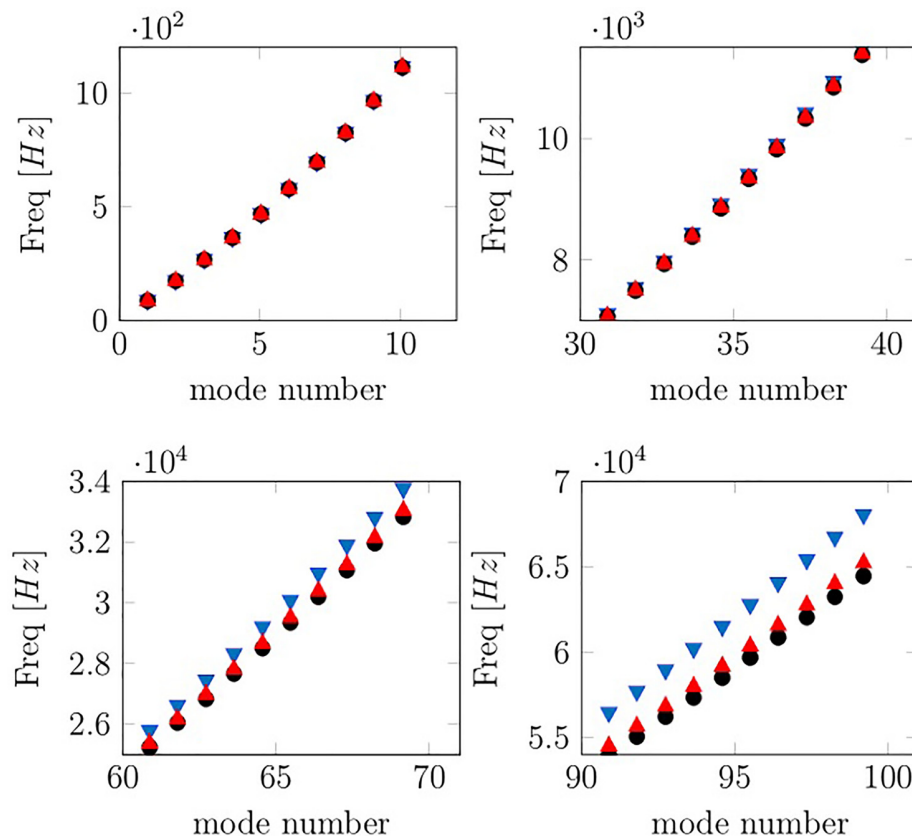


FIG. 4. (Color online) Eigenfrequencies for the E_2^g string under clamped boundary conditions for Timoshenko (circles), shear (upward triangles), Euler–Bernoulli (downward triangles), for different modal numbers.

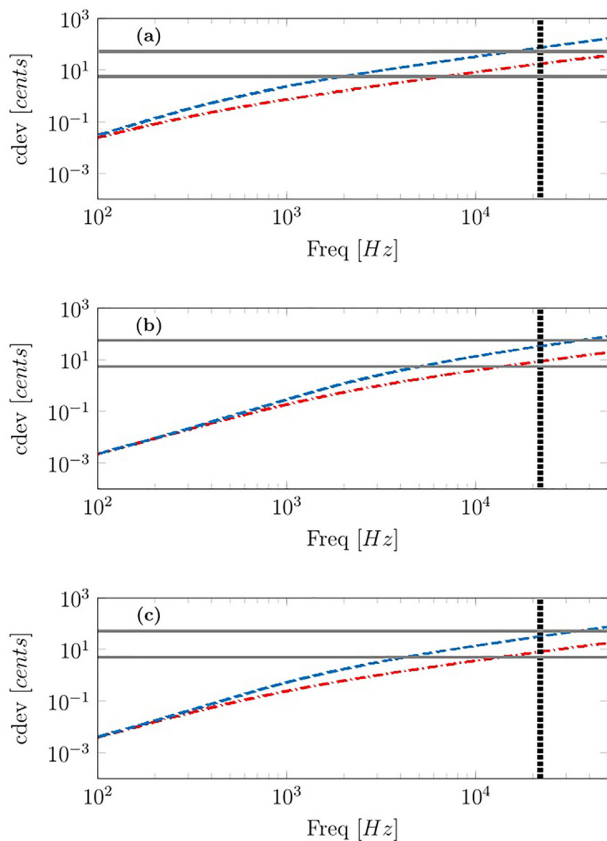


FIG. 5. (Color online) Deviations in cents under simply supported boundary conditions, for (a) E_1^b ; (b) $D_{\#1}^p$; (c) E_2^g . In the figures, SH is represented by a dashed-dotted line, EB by a dashed line. The vertical dashed lines represent the limit of human hearing (20 kHz) and the horizontal solid lines represent the 5 and 50 cents limits.

large frequency range, for simply supported boundary conditions. The three plots correspond to the three strings E_1^b , $D_{\#1}^p$, E_2^g . The limit of human hearing (20 kHz) is marked with a vertical dashed line; the two horizontal lines are the 5 and 50 cents boundaries. It is seen that, as expected, E_1^b is the string which shows a larger deviation, and also the string for which deviation sets in at smaller frequencies compared to the other two models. Deviation in cents at the limit of hearing are not dissimilar from those already given for the dispersion curves, in Sec. VIA. Basically, the Euler–Bernoulli model deviates by about half a semitone at the limit of human hearing, for the bass string, whereas the shear model deviates by about a quarter of that. In addition, note that, for the bass, the 5 cents boundary is overtaken at about 2 kHz for the Euler–Bernoulli model and 7 kHz for the shear model. For the piano and guitar strings, such boundary is overtaken at around 4 kHz for the Euler–Bernoulli model and above 10 kHz for the shear model.

It is worth recalling that for the strings under consideration stiffness effects are at the extreme, and that for slender strings a better match is expected.

VII. DISCUSSION AND CONCLUSIONS

Three linear string models were presented, assessed and evaluated in cases of interest in musical acoustics. All these

models take into account stiffness, which is responsible for various important perceptual effects. Previous works have made extensive use of the Euler–Bernoulli model, because of its simple form. However, in the limit of large wavenumbers the phase and group velocities attain infinity, and such behaviour has been regarded by a few as unphysical. The other prominent model in the literature, the Timoshenko model, has bounded group velocity. Here a third model was introduced in the context of musical acoustics, based on the shear model for beams.

In this paper, it was shown that not only does the shear model present bounded phase and group velocities, but the asymptotes at infinity are the same as for the lower branch of the Timoshenko system. The shear model presents a simpler mathematical formulation than the Timoshenko model. In particular, when the system is written in the sole transverse displacement w , the shear model is of order 2 in time, whereas the Timoshenko model is of order 4, thus requiring the specification of four initial conditions. As a consequence of that, the upper branch of the Timoshenko system is not reproduced by the shear model. However, for musical acoustics this is not a limitation as it such a branch was shown to lie well above the audible range.

All three models show good agreement at low frequencies, with the dispersion relations attaining the same limit.

The modal frequencies reflect the behaviour already noted for the dispersion curves; hence extremely good match for lower modes and increasing deviation as the mode number increases. Again, deviations are more prominent for the Euler–Bernoulli model than for the shear model, with the latter presenting maximum deviations of less than 1 semitone for all the case studies. It is as well worth noticing that, because the deviations grow monotonically with the mode number, for large portions of the audible spectrum both the Euler–Bernoulli and shear models present negligible deviations from the Timoshenko system.

The results in this paper show that the shear model can be used as a very satisfying alternative to the Timoshenko model. In view of a numerical application, the shear model can be used in its compact form Eq. (6), which includes the effect of the constraint due to the shear deformation.

On the other hand, the popularity of the Euler–Bernoulli model finds here further justification, especially if one is interested in analysing and possibly simulating slender strings than those presented here as case studies; if at high frequencies the Euler–Bernoulli model may produce perceptually noticeable differences, for large parts of the spectrum the deviations remain very small.

ACKNOWLEDGMENTS

This work was supported by the European Research Council, under grant number StG-2011-279068-NESS, and by the Royal Society and the British Academy, through a Newton International Fellowship.

APPENDIX: COEFFICIENTS FOR THE FREQUENCY EQUATIONS IN TABLE III

A. Timoshenko's model

$$\begin{aligned}
 C_{cl} &= C_{cl}^N / C_{cl}^D; \\
 C_{cl}^N &= \beta^2(\lambda_-^2 - \lambda_+^2)\omega^4 + (\beta(\lambda_- - \lambda_+)(\beta(\lambda_+^3 - \lambda_-^3)\alpha \\
 &\quad + \lambda_- + \lambda_+) - \beta(\lambda_- + \lambda_+)(\beta(\lambda_-^3 + \lambda_+^3)\alpha \\
 &\quad + \lambda_+ - \lambda_-))\omega^2 - \beta(\lambda_+^3 - \lambda_-^3)\alpha + \lambda_- + \lambda_+ \\
 &\quad \times (\beta(\lambda_-^3 + \lambda_+^3)\alpha + \lambda_+ - \lambda_-); \\
 C_{cl}^D &= 2\lambda_- \lambda_+ (\alpha\beta\lambda_+^2 + \beta\omega^2 + 1)(\alpha\beta\lambda_-^2 - \beta\omega^2 - 1). \\
 C_{ff} &= C_{ff}^N / C_{ff}^D; \\
 C_{ff}^N &= -(\alpha + \beta)(\lambda_- + \lambda_+)\omega^4 + (\alpha(\lambda_- + \lambda_+) - \lambda_+ - \lambda_- \\
 &\quad + \alpha\beta(\lambda_- + \lambda_+)^2(\lambda_- - \lambda_+) + \alpha^2\lambda_- \lambda_+(\lambda_- - \lambda_+))\omega^2 \\
 &\quad + \alpha\lambda_- \lambda_+(\lambda_- - \lambda_+ + \alpha(\lambda_+ - \lambda_- + \beta\lambda_- \lambda_+ \\
 &\quad \times (\lambda_- + \lambda_+))); \\
 C_{ff}^D &= 2\lambda_- \lambda_+ (\alpha\lambda_-^2 - \omega^2)(\alpha\lambda_+^2 + \omega^2) \\
 &\quad \times (\alpha\omega^2 - \alpha + \beta\omega^2 - \alpha\beta\lambda_-^2 + 1) \\
 &\quad \times (\alpha\omega^2 - \alpha + \beta\omega^2 + \alpha\beta\lambda_+^2 + 1).
 \end{aligned}$$

B. Shear model

$$\begin{aligned}
 C_{cl} &= C_{cl}^N / C_{cl}^D; \\
 C_{cl}^N &= \beta(\lambda_+^2 - \lambda_-^2)\omega^4 + 2\beta(\alpha\beta(\lambda_-^4 + \lambda_+^4) - \lambda_-^2 + \lambda_+^2)\omega^2 \\
 &\quad - \alpha\beta(\alpha\beta(\lambda_-^6 + \lambda_+^6) + 2\lambda_-^4 + 2\lambda_+^4) - \lambda_-^2 + \lambda_+^2; \\
 C_{cl}^D &= 2\lambda_- \lambda_+ (-\alpha\beta\lambda_-^2 + \beta\omega^2 + 1)(\alpha\beta\lambda_+^2 + \beta\omega^2 + 1). \\
 C_{ff} &= C_{ff}^N / C_{ff}^D; \\
 C_{ff}^N &= (\beta(\lambda_- - \lambda_+)\omega^4 - (\lambda_- - \lambda_+)(\alpha\beta\lambda_-^2 - \alpha\beta\lambda_+^2 \\
 &\quad + \alpha - 1)\omega^2 - \alpha\lambda_- \lambda_+(\alpha\lambda_- - \lambda_+ - \lambda_- + \alpha\lambda_+ \\
 &\quad - \alpha\beta\lambda_- \lambda_+^2 + \alpha\beta\lambda_-^2 \lambda_+))(-\beta(\lambda_- + \lambda_+)\omega^4 \\
 &\quad + (\lambda_- + \lambda_+)(\alpha\beta\lambda_-^2 - \alpha\beta\lambda_+^2 + \alpha - 1)\omega^2 \\
 &\quad + \alpha\lambda_- \lambda_+(\lambda_- - \lambda_+ - \alpha\lambda_- + \alpha\lambda_+ + \alpha\beta\lambda_- \lambda_+^2 \\
 &\quad + \alpha\beta\lambda_-^2 \lambda_+)); \\
 C_{ff}^D &= 2\lambda_- \lambda_+ (\alpha\lambda_-^2 - \omega^2)(\alpha\lambda_+^2 + \omega^2) \\
 &\quad \times (\alpha\beta\lambda_-^2 - \beta\omega^2 + \alpha - 1)(\alpha\beta\lambda_+^2 + \beta\omega^2 - \alpha + 1).
 \end{aligned}$$

C. Euler-Bernoulli model

$$\begin{aligned}
 C_{cl} &= (\lambda_+^2 - \lambda_-^2) / (2\lambda_- \lambda_+); \\
 C_{ff} &= C_{ff}^N / C_{ff}^D; \\
 C_{ff}^N &= (\lambda_- + \lambda_+)\alpha + \beta\lambda_- \lambda_+(\lambda_- - \lambda_+) - \lambda_- - \lambda_+ \\
 &\quad \times (\lambda_+ - \lambda_- + \alpha(\lambda_- - \lambda_+) - \beta\lambda_- \lambda_+(\lambda_+ - \lambda_-)); \\
 C_{ff}^D &= 2\lambda_- \lambda_+ (\beta\lambda_-^2 + \alpha - 1)(\beta\lambda_+^2 - \alpha + 1).
 \end{aligned}$$

- ¹S. Bilbao, *Numerical Sound Synthesis: Finite Difference Schemes and Simulation in Musical Acoustics* (Wiley, Chichester, UK, 2009), Chap. 6.
- ²P. Ruiz, "A technique for simulating the vibrations of strings with a digital computer," Master's thesis, University of Illinois, 1969.
- ³L. Hiller and P. Ruiz, "Synthesizing musical sounds by solving the wave equation for vibrating objects: Part I," *J. Audio Eng. Soc.* **19**(6), 462–470 (1971).
- ⁴R. A. Bacon and J. M. Bowsher, "A discrete model for of the struck string," *Acustica* **41**, 21–27 (1978).
- ⁵X. Boutillon, "Model for piano hammers: Experimental determination and digital simulation," *J. Acoust. Soc. Am.* **83**(2), 746–754 (1988).
- ⁶A. Chaigne and A. Askenfelt, "Numerical simulations of piano strings 1. A physical model for a struck string using finite difference methods," *J. Acoust. Soc. Am.* **95**(2), 1112–1118 (1994).
- ⁷N. Giordano, "Finite difference modeling of the piano," *J. Acoust. Soc. Am.* **119**(5), 3291–3291 (2006).
- ⁸J. Bensa, S. Bilbao, R. Kronland-Martinet, and J. O. Smith, "The simulation of piano string vibration: From physical models to finite difference schemes and digital waveguides," *J. Acoust. Soc. Am.* **114**(2), 1095–1107 (2003).
- ⁹E. Ducasse, "On waveguide modeling of stiff piano strings," *J. Acoust. Soc. Am.* **118**(3), 1776–1781 (2005).
- ¹⁰K. F. Graff, *Wave Motion in Elastic Solids* (Dover, New York, 1991), Chap. 3.
- ¹¹J. Chabassier and S. Imperiale, "Stability and dispersion analysis of improved time discretisation for prestressed Timoshenko systems. Application to the stiff piano string," *Wave Motion* **50**, 456–480 (2013).
- ¹²J. Chabassier, A. Chaigne, and P. Joly, "Modeling and simulation of a grand piano," *J. Acoust. Soc. Am.* **134**(1), 648–665 (2013).
- ¹³J. Chabassier, A. Chaigne, and P. Joly, "Time domain simulation of a piano. Part 1: Model description," *ESAIM: Math. Model. Numer. Anal.* **45**, 1241–1278 (2013).
- ¹⁴H. Fletcher, "Normal vibration frequencies of a stiff piano string," *J. Acoust. Soc. Am.* **36**(1), 203–209 (1964).
- ¹⁵S. M. Han, H. Benaroya, and T. Wei, "Dynamics of transversely vibrating beams using four engineering theories," *J. Sound Vib.* **225**(3), 935–988 (1999).
- ¹⁶G. Jelenić and M. A. Crisfield, "Geometrically exact 3D beam theory: Implementation of a strain-invariant finite element for statics and dynamics," *Comp. Methods Appl. Mech. Eng.* **171**, 141–171 (1999).
- ¹⁷P. Betsch and P. Steinmann, "Frame-indifferent beam finite elements based upon the geometrically exact beam theory," *Int. J. Numer. Methods Eng.* **54**(12), 1775–1788 (2002).
- ¹⁸R. W. Traill-Nash and A. R. Collar, "The effect of shear flexibility and rotary inertia on the bending vibrations of beams," *Q. J. Mech. Appl. Math.* **6**(2), 186–222 (1953).
- ¹⁹R. Davis, R. D. Henshell, and G. B. Warburton, "A Timoshenko beam element," *J. Sound Vib.* **22**(4), 475–487 (1972).
- ²⁰J. D. Renton, "Check on the accuracy of Timoshenko's beam theory," *J. Sound Vib.* **245**(3), 559–561 (2001).
- ²¹N. G. Stephen, "On a check on the accuracy of Timoshenko's beam theory," *J. Sound Vib.* **257**(4), 809–812 (2002).
- ²²A. N. Kounadis, "On the derivation of the equations of motion for a vibrating Timoshenko column," *J. Sound Vib.* **73**(2), 177–184 (1980).
- ²³K. Sato, "On the governing equations for vibration and stability of a Timoshenko beam: Hamilton's principle," *J. Sound Vib.* **145**(2), 338–340 (1991).
- ²⁴P. A. Djondjorov and V. M. Vassilev, "On the dynamic stability of a cantilever under tangential follower force according to Timoshenko beam theories," *J. Sound Vib.* **311**, 1431–1437 (2008).
- ²⁵D. Hodges, "Asymptotic derivation of shear beam theory from Timoshenko theory," *J. Eng. Mech.* **133**(8), 957–961 (2007).
- ²⁶J. Aristizabal-Ochoa, "Discussion of asymptotic derivation of shear beam theory from Timoshenko theory by Dewey H. Hodges," *J. Eng. Mech.* **135**(4), 361–362 (2009).
- ²⁷E. Kausel, "Nonclassical modes of unrestrained shear beams," *J. Eng. Mech.* **128**(6), 663–667 (2002).